

Sub-nanosecond single-frequency 10-kHz diode-pumped MOPA laser

A. Agnesi · P. Dallochio · F. Pirzio · G. Reali

Received: 8 July 2009 / Revised version: 15 September 2009 / Published online: 12 November 2009
© Springer-Verlag 2009

Abstract A single-axial-mode, passively Q-switched (PQS) diode-pumped Nd:YAG laser, generating a diffraction-limited beam train of $\approx 40\text{--}60\ \mu\text{J}$, $\sim 500\text{-ps}$ pulses with adjustable repetition rate in the range 1–10 kHz, was efficiently amplified by a single side-pumped Nd:YVO₄ bounce amplifier. After double-pass amplification, $\approx 1\text{-MW}$ pulse peak power with 577-ps duration and 545- μJ energy was achieved, still maintaining diffraction-limited beam performance. The average output power was 5.45 W at 10 kHz, corresponding to 13% extraction efficiency. The high brightness of this laser system seems ideal for nonlinear optics and some particular laser processing applications.

PACS 42.55.Xi · 42.60.Gd · 42.60.-v

1 Introduction

Many applications such as harmonic and parametric conversion, generation of THz waves, and laser processing of transparent materials, can take advantage of relatively short ($< 1\ \text{ns}$) high peak power ($\approx 1\ \text{MW}$) laser pulses.

Indeed, given the peak intensity required for efficiently activating some nonlinear optical processes, the intensity damage threshold scaling as $\sim \tau_p^{1/2}$ for most optical materials favors pulses with shorter duration τ_p [1]. Also, laser writing within transparent materials is made easier with shorter pulses, leading to more effective multi-photon absorption and confined, local damaging rather than extended

damaging associated to thermal shocks as it is usually observed in the multi-ns pulse regime.

It is also worth noticing that multi-kHz pulse operation is most often desirable for industrial material processing.

Few remarkable examples of diode-pumped solid-state lasers with pulse duration $\leq 1\ \text{ns}$ and peak power $\sim 1\ \text{MW}$ have been reported recently.

A 237-ps PQS composite Yb:YAG/Cr⁴⁺:YAG microchip laser was shown to operate at a maximum frequency of 3.5 kHz with 175 μJ pulse energy and 0.7-MW peak power [2]. The intracavity peak intensity in this case was $\approx 36\ \text{GW}/\text{cm}^2$, and optical damage is clearly the major challenge for this kind of laser system.

A 420-ps, $\approx 1\text{-MW}$ oscillator was also demonstrated with a PQS unstable resonator [3]. The ability of such a resonator to manage a large mode area without compromising the beam quality allows for much safer energy scaling, but the high loss required for high-energy and short-pulse Q-switching translate to a very high laser threshold and parasitic thermal effects, which eventually inhibit high-frequency operation above $\approx 200\ \text{Hz}$.

Multi-kHz operation with an amplified low-power microchip was reported by Forget et al. [4]: an 800-ps 3.9- μJ microchip laser PQS at 28 kHz was amplified in a 3D multi-pass geometry (up to 8 passes) with either Nd:YAG or Nd:YVO₄ diode-pumped crystals. As much as 5.7 W was achieved at 500-ps pulse duration (0.4-MW peak power).

A different approach relying on a moderate-energy high-frequency oscillator and a single high-gain amplifier stage with only one or two passes looks more straightforward, flexible and power-scalable. Side-pumped Nd:YVO₄ bounce amplifiers [5–9] have been proved to be an excellent design solution for achieving high gains in a single pass (up to 40 dB, depending on the pump focusing), thus allowing

A. Agnesi (✉) · P. Dallochio · F. Pirzio · G. Reali
INFN Sezione di Pavia and Dipartimento di Elettronica,
dell'Università di Pavia, Via Ferrata 1, 27100 Pavia, Italy
e-mail: antonio.agnesi@unipv.it
Fax: +39-382-422583

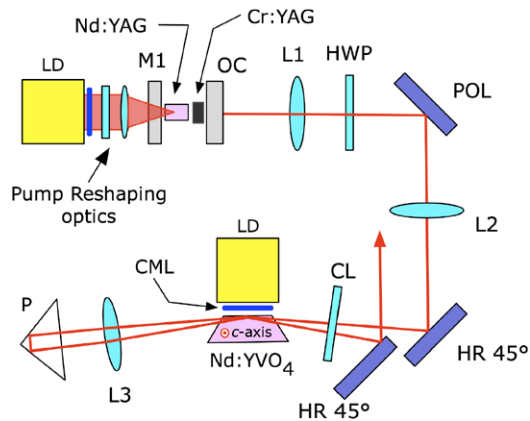


Fig. 1 Laser setup. LDs: pump laser diodes (40-W linear arrays), fast-axis collimated with cylindrical microlens (CML). The PQS oscillator includes the input mirror M1 (concave, $r = 1$ m) and the 30%-reflectivity output coupler OC. L1: collimating lens (75-mm focal); HWP: $\lambda/2$ plate; POL: 45° polarizer; L2: 300-mm focal lens; CL: cylindrical lens (75-mm focal); L3: spherical lens (100-mm focal); P: right-angle prism. The Nd:YVO₄ slab is a -cut with vertical c -axis, parallel to pump diode polarization

for a significant power extraction with a compact and simple setup.

We report here on a ≈ 577 -ps PQS multi-kHz laser system in a Master Oscillator Power Amplifier (MOPA) configuration, with a maximum average output power of 5.45 W and a peak power ≈ 1 MW at 10 kHz, in a diffraction-limited, single-axial frequency beam.

2 Experiment

The master oscillator was a PQS Cr⁴⁺:YAG/Nd:YAG laser (Fig. 1), longitudinally pumped by a 40-W diode laser array driven at ≈ 40 - μ s 40-A current pulses, properly reshaped to deliver an approximately circular pump spot of ≈ 170 μ m diameter and $M^2 \approx 43$ in both directions. By a proper choice of the Cr⁴⁺:YAG unsaturated transmission (40%) and output coupling (30%), the 7-mm long, plain-concave resonator (with end-mirror curvature radius = 1000 mm) generated 62- μ J, ≈ 473 -ps pulses at 10 kHz. The TEM₀₀ resonant spatial mode (of ≈ 70 μ m measured waist radius) was mainly shaped by the gain profile [3], the concave mirror being chosen only to help resonator alignment. Indeed, the resonator cavity was very short for significant thermal lensing and the measured resonant-mode radius did not change appreciably in the range 1–10 kHz. In comparison with Ref. [3] specifications, a lower pump threshold was required for laser oscillation owing to the reduced losses and the tighter pump focussing, resulting from the higher beam quality of the reshaped diode array. This eventually allowed us to upscale the repetition frequency in the multi-kHz regime.

Diffraction-limited, single longitudinal-mode (SLM) operation was observed up to the maximum repetition frequency of 10 kHz. Slightly above 12 kHz the oscillator became unstable, and turned off after few minutes. By slightly increasing the pump energy, the laser operation could be restored, but it eventually went down again after few minutes. This is exactly the same behavior as we observed, at a lower frequency, with the PQS oscillator of Ref. [3]. Since the beam profile did not change under these limiting conditions, as it would happen with an onset of excessive thermal lensing producing resonator instability, we suggest that other “slow” parasitic thermal effects take place instead. These are usually due to pump power dissipation through quantum defect and possibly upconversion effects, yielding thermally-induced spectral gain broadening and emission cross section reduction [10], eventually leaving too low a gain to overcome losses at a sufficiently high repetition frequency.

Owing to the good overlap between Nd:YAG and Nd:YVO₄ gain bandwidths we designed a compact grazing-incidence Nd:YVO₄ amplification stage.

The amplification medium was an a -cut $4 \times 2 \times 15$ mm³, 1% doped, 6° wedged slab with input and output beam faces antireflection-coated (AR) at 1064 nm and with the pumped side AR-coated at 808 nm. The slab was pumped by a 40-W cw diode laser array vertically polarized parallel to the slab’s c -axis, tuned at 808 nm and collimated by a cylindrical microlens CML (Fig. 1), yielding a gain sheet of ≈ 200 μ m in the vertical direction. The depth of the gain sheet in the horizontal plane is basically determined by the pump absorption depth, $1/\alpha p \approx 0.5$ mm, given the pump spectral width and the chosen Nd:YVO₄ doping concentration. The 4×15 mm² faces of the slab were placed in contact, by thin indium foils, with a water-cooled heat exchanger. In order to optimize the energy extraction and to reduce the thermal aberrations, both the incidence angle and the seed beam waist inside the amplifier medium must be properly controlled. A good mode matching between the injected seed and elliptical cross section $\approx 0.5 \times 0.2$ mm² of the gain sheet was then required. As shown in Fig. 1, the spherical lens L2 (300-mm focal) focussed the oscillator beam in the slab to match the horizontal gain diameter, whereas a cylindrical lens CL (75-mm focal) provided additional focussing in the vertical plane. The grazing angle has been chosen to be as small as possible in order to maximize the gain while avoiding clipping effects.

Double-pass amplification was realized by re-imaging the single-pass output with a spherical lens L3 (100-mm focal) and a right-angle AR-coated prism P, thus maintaining the same spot size as in the first pass, but with a slightly different grazing angle $\approx 2^\circ$ larger. Beam extraction occurred after the lens CL.

Both the average output power and the pulse energy were maximized at 10 kHz. Fig. 2 shows the gain and the out-

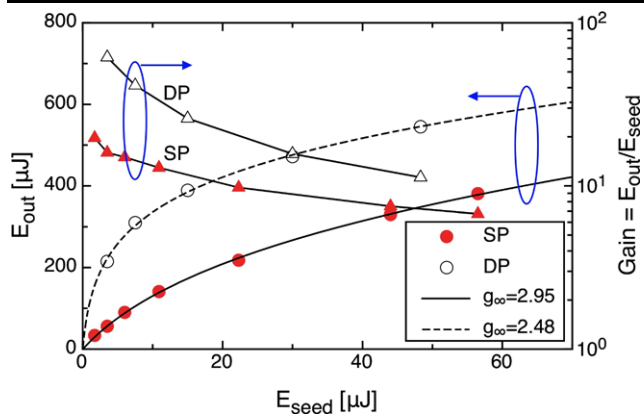


Fig. 2 Single-pass (SP) and double-pass (DP) gain and output energy as a function of the seed pulse energy at 10 kHz

put energy E_{out} at 10 kHz, as a function of the seed energy E_{in} that was allowed to be changed by a variable attenuator. These curves have been fitted to the standard model of the laser amplifier [1, 11], allowing one to determine the small-signal low-frequency exponential gain g_{∞} and the saturation energy E_{sat} :

$$E_{out} = E_{sat} \ln[1 + (e^{E_{in}/E_{sat}} - 1)e^{g_i}] \tag{1}$$

$$g_i = g_{\infty} - (g_{\infty} - g_f) e^{-\frac{1}{f\tau}} \tag{2}$$

$$E_{out} = E_{in} + (g_i - g_f) E_{sat} \tag{3}$$

Here g_i is the small-signal gain before the pulse amplification, g_f is the residual gain that is restored to g_i by the cw pump, $\tau \approx 100 \mu s$ is the fluorescence lifetime and f is the pulse repetition frequency. We notice that $g_{\infty} = g_i$ when $f \rightarrow 0$ [1].

Equations (1–3) apply to single-pass amplification, while sequential application of the same model readily accounts for the double-pass scheme with no temporal overlapping of the pulses within the amplifier [12].

Comparing single- and double-pass results, it turns out that the exponential small-signal gain is higher at 10 kHz ($g_{\infty}^{(SP)} = 2.95, g_{\infty}^{(DP)} = 2.48$) than at 1 kHz ($g_{\infty}^{(SP)} = 2.55, g_{\infty}^{(DP)} = 2.10$). This can be explained by the slight wavelength mismatch between the oscillator pulse and the fluorescence line of the amplifier: it is known that the Nd:YAG fluorescence peak shifts $\approx +4 \text{ pm}/^{\circ}\text{C}$ [10], so at a higher repetition rate the seed pulse experiences a higher emission cross section in the amplifier (at room temperature the fluorescence peaks of Nd:YAG and Nd:YVO₄ are 1064.1 nm and 1064.3 nm, respectively [1]).

We also note that $g_{\infty}^{(DP)} < g_{\infty}^{(SP)}$ since in the double-pass setup the backward path follows a larger grazing angle (with smaller gain); hence the single parameter g_{∞} used to model the double-pass amplifier is necessarily smaller. Of course, what really counts is the total small-signal gain $2 \times g_{\infty}^{(DP)}$ or

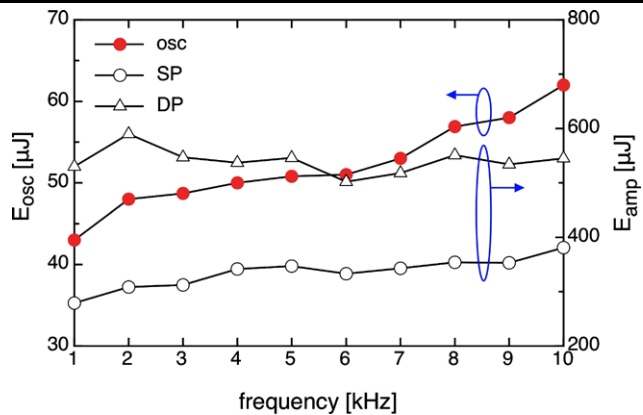


Fig. 3 Output energy from the oscillator and after single- and double-pass amplification (SP, DP), as a function of the repetition frequency

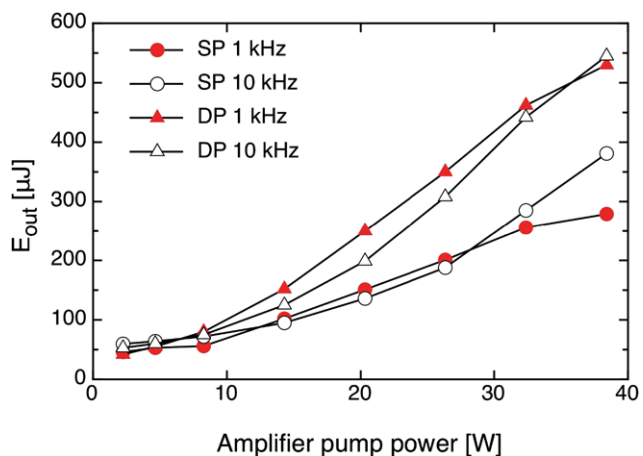


Fig. 4 Single- and double-pass (SP, DP) output energy as a function of the pump power incident (and almost completely absorbed) on the Nd:YVO₄ slab amplifier

the sum of forward and backward g_{∞} if they were considered separately (which would give the same final result).

Figure 3 shows the variation of the oscillator pulse energy with the frequency, as well as the amplified output (single- and double-pass). The increase of pulse energy is basically determined by the increasing temperature of the Nd:YAG crystal at higher pump rates, as observed in Ref. [10]. Indeed, the thermal lens in our oscillator does not change significantly the beam focussing in the saturable absorber. However, owing to amplifier saturation, the output energy showed a less marked trend with the repetition frequency, especially in the double-pass setup.

As shown in Fig. 4, as much as 3.81 W in single-pass and 5.45 W in double-pass at 10 kHz was obtained with 38.4-W pump power, corresponding to an extraction efficiency $\approx 13\%$. Given the setup simplicity, this result compares favorably with that of a previously reported monolithic MOPA with relatively short 5-ns pulses at 10 kHz

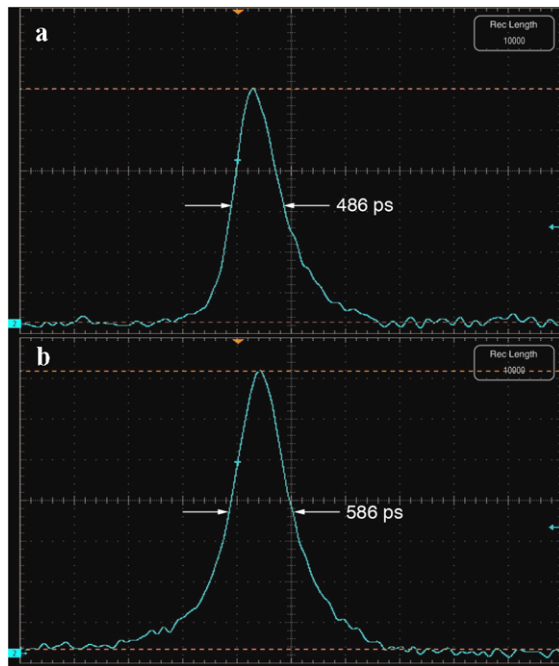
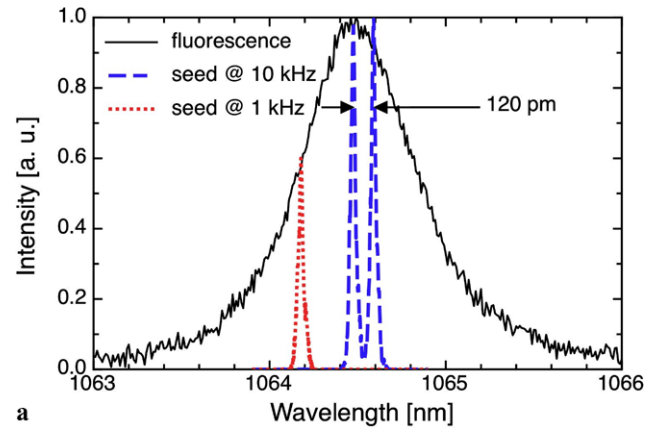


Fig. 5 Input and output pulse traces at 10 kHz

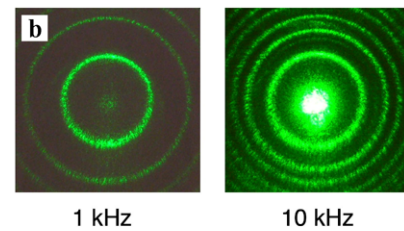
(energy extraction 13% [13]) while other bounce amplifiers with much longer nanosecond pulses and MHz repetition rate have reached an efficiency as high as 44% [7]. Clearly, tighter focussing of the diode array into the slab readily increases the gain and would improve the performance accordingly, but in our case we needed to trade off amplifier efficiency with damage-free operation. In facts, the peak intensity was estimated to be 2 GW/cm^2 , approaching the nominal damage threshold of the AR coatings at 1064 nm for 500 ps pulses ($\approx 500 \text{ MW/cm}^2$ for 10 ns pulses).

The beam quality of the MOPA system was measured with a CCD camera, with the amplifier either switched off ($M_x^2 \times M_y^2 = 1.1 \times 1.0$) or switched on at full pump power ($M_x^2 \times M_y^2 = 1.2 \times 1.0$). Only the two-pass result was measured, since this brings about the stronger thermal aberration, and beam quality deterioration is more apparent. No significant worsening with respect to the TEM_{00} seeder profile was observed. A 6-GHz oscilloscope (Tektronix TDS 6604B) and a 5-GHz photodiode (Thorlabs SIR5-FC) were employed for pulse measurement, and the detection system pulse response ($\approx 100 \text{ ps}$) was deconvolved from the pulse width displayed by the oscilloscope. The amplified pulse width ($\approx 577 \text{ ps}$, Fig. 5) was slightly longer than that of the PQS oscillator ($\approx 473 \text{ ps}$), while in single-pass amplification the two pulse widths were nearly identical.

The anticipated thermal shift of the oscillator wavelength is clearly evidenced in Fig. 6, which also shows the double-axial-mode operation at 10 kHz. This effect might also be used to measure indirectly the average axial temperature inside the Nd:YAG crystal. However, the pulses are still SLM



a



1 kHz

10 kHz

Fig. 6 **a** Seed spectra at 1 kHz, 10 kHz and fluorescence spectra of the Nd:YVO₄ slab pumped at 38.4 W. **b** Ring patterns of the longitudinal modes from a 1 mm etalon (finesse ≈ 60) after second harmonic generation at 532 nm. The spectrum at 10 kHz shows twice the rings visible at 1 kHz, with no significant sum frequency, thus proving that the single Q-switched pulse is SLM

at 10 kHz. This is clearly proved by the ring patterns produced (after second harmonic generation with an LBO crystal) by a 1-mm thick fused silica etalon, with 95% reflectivity at 532 nm of both the end-faces: if a laser pulse had two axial frequencies ω_1 and ω_2 , a second harmonic would produce a spectrum with three frequencies of comparable intensity, i.e. $2\omega_1$, $2\omega_2$ and $\omega_1 + \omega_2$. Instead, the ring pattern at 10 kHz shows only twice the ring count at 1 kHz, therefore each pulse is only responsible for either $2\omega_1$ or $2\omega_2$. It is worth noticing that the dual-mode separation is $\approx 120 \text{ pm}$, i.e. two free-spectral ranges of the oscillator cavity. This suggests that, starting from 2–3 kHz repetition rates, the mode near the gain peak of Nd:YAG stops lasing in favor of its neighbors, which run one at a time in each alternate pulse (as confirmed by using two photodiodes and displaying the pulse train of two adjacent rings on the oscilloscope).

One possible reason of this behavior might be that at repetition rates approaching $1/\tau$, making the population inversion modulation smaller [1], a stronger Cr:YAG saturation and lower intracavity losses could be achieved by laser frequency off-peak self-adjusting where the ratio between absorption and emission cross sections increases, thus yielding a more effective PQS.

3 Conclusions

We have demonstrated a MOPA laser system generating intense ~ 500 -ps SLM pulses with energy exceeding $500 \mu\text{J}$ at 1–10 kHz, with diffraction-limited beam quality. Large-area photonic fiber amplifiers have also demonstrated generation of milli-Joule sub-ns pulses [14], though such fibers are not yet readily available as commercial components with demonstrated long lifetimes. Furthermore, the pulse spectrum of high energy fiber lasers is most often highly structured owing to intense nonlinear interactions, and this may be an issue for some applications.

On the other hand, the proposed approach clearly shows the potential of scaling this architecture toward higher pulse energy. The intensity level currently available makes this MOPA system particularly attractive for nonlinear optical applications, such as optical parametric generation and harmonic conversion [15], as well as sum/difference frequency generation, especially concerning the THz domain [16].

Acknowledgements We acknowledge the contribution of Bright Solutions, Srl, for supporting and discussion. This research received funding from the European Community's Seventh Framework Programme FP7/2007-2011 under grant agreement n°224042.

References

1. W. Koechner, *Solid-State Laser Engineering* (Springer, Berlin, 2006)
2. J. Dong, K. Ueda, A. Shirakawa, H. Yagi, T. Yanagitani, A. Kaminskii, *Opt. Express* **15**, 14516 (2007)
3. A. Agnesi, F. Pirzio, G. Reali, G. Piccinno, *Appl. Phys. Lett.* **89**, 101120 (2006)
4. S. Forget, F. Balembois, P. Georges, P.-J. Devilder, *Appl. Phys. B* **75**, 481 (2002)
5. J.E. Bernard, A.J. Alcock, *Opt. Lett.* **18**, 968 (1993)
6. A. Minassian, B. Thompson, M.J. Damzen, *Appl. Phys. B* **76**, 341 (2003)
7. S.P. Chard, M.J. Damzen, *Opt. Express* **17**, 2218 (2009)
8. A. Agnesi, L. Carrà, F. Pirzio, G. Reali, A. Tomaselli, D. Scarpa, C. Vacchi, *IEEE J. Quantum Electron.* **42**, 772 (2006)
9. A. Agnesi, P. Dallochio, L. Carrà, F. Pirzio, G. Reali, A. Tomaselli, D. Scarpa, C. Vacchi, *IEEE J. Quantum Electron.* **44**, 952 (2008)
10. O. Kimmelma, I. Tittonen, S.C. Buchter, *Appl. Opt.* **47**, 4262 (2008)
11. L.M. Franz, J.S. Nodvik, *J. Appl. Phys.* **34**, 2346 (1963)
12. S. Pearce, C.L.M. Ireland, P.E. Dyer, *Opt. Commun.* **255**, 297 (2005)
13. Z. Ma, D. Li, P. Hu, A. Shell, P. Shi, C.R. Haas, N. Wu, K. Du, *Opt. Lett.* **32**, 1262 (2007)
14. F. di Teodoro, C.D. Brooks, *Opt. Lett.* **30**, 2694 (2005)
15. J.J. Zayhowski, *IEEE Photon. Tech. Lett.* **9**, 925 (1997)
16. G.Kh. Kitaeva, *Laser Phys. Lett.* **5**, 559 (2008)